

Adenosine is crucial for deep brain stimulation–mediated attenuation of tremor

Lane Bekar^{1,3}, Witold Libionka^{1,3}, Guo-Feng Tian¹, Qiwu Xu¹, Arnulfo Torres¹, Xiaohai Wang¹, Ditte Lovatt¹, Erika Williams¹, Takahiro Takano¹, Jurgen Schnerrmann², Robert Bakos¹ & Maiken Nedergaard¹

Deep brain stimulation (DBS) is a widely used neurosurgical approach to treating tremor and other movement disorders^{1–3}. In addition, the use of DBS in a number of psychiatric diseases, including obsessive-compulsive disorders and depression, is currently being tested^{4–6}. Despite the rapid increase in the number of individuals with surgically implanted stimulation electrodes, the cellular pathways involved in mediating the effects of DBS remain unknown¹. Here we show that DBS is associated with a marked increase in the release of ATP, resulting in accumulation of its catabolic product, adenosine. Adenosine A1 receptor activation depresses excitatory transmission in the thalamus and reduces both tremor- and DBS-induced side effects. Intrathalamic infusion of A1 receptor agonists directly reduces tremor, whereas adenosine A1 receptor–null mice show involuntary movements and seizure at stimulation intensities below the therapeutic level. Furthermore, our data indicate that endogenous adenosine mechanisms are active in tremor, thus supporting the clinical notion that caffeine, a nonselective adenosine receptor antagonist, can trigger or exacerbate essential tremor⁷. Our findings suggest that nonsynaptic mechanisms involving the activation of A1 receptors suppress tremor activity and limit stimulation-induced side effects, thereby providing a new pharmacological target to replace or improve the efficacy of DBS.

To show that high-frequency stimulation (HFS) results in ATP release, we used a bioluminescence technique⁸, in which thalamic slices (postnatal day 18–21) are perfused with a solution containing a mixture of luciferase and D-luciferin. The photons emitted after ATP catalyzes the oxidation of D-luciferin are imaged by a liquid nitrogen-cooled charge-coupled device camera⁹. HFS triggered an abrupt increase in extracellular ATP around the stimulation electrode, which is sensitive to the polarity of stimulation (Fig. 1a). Consistent with the idea that only cathodic stimulation suppresses tremor activity^{10,11}, the cathode gave rise to five- to tenfold higher ATP release than occurred when the polarity was changed and the same electrode delivered positive (anodic) stimulation (Fig. 1b). ATP release was a direct function of the current amplitude and the frequency of stimulation

(Fig. 1c). Experiments on exposed mouse cortices *in vivo* closely followed the same frequency- and amplitude-dependent pattern of ATP release detected in thalamic slices (Supplementary Fig. 1 online). Removal of extracellular Ca²⁺ from the bath solution in the slice experiments (to prevent synaptic release of ATP) resulted in enhanced ATP bioluminescence, indicating that ATP release was primarily nonsynaptic and probably resulted from an efflux of cytosolic ATP (Fig. 1d). As it is known that astrocytic Ca²⁺ waves are mediated by ATP and P2Y receptors, we assessed astrocytic Ca²⁺ responses to HFS in live mouse cortex^{12,13}. Not unexpectedly, we found that HFS induced astrocytic Ca²⁺ waves that propagated away from the site of stimulation in a frequency- and amplitude-dependent manner (Supplementary Fig. 1)¹⁴. Thus, both direct bioluminescence and indirect calcium measures of ATP release in response to HFS depict a pattern that correlates directly with effective clinical stimulation parameters.

As ATP is degraded to adenosine by extracellular ectonucleotidases with a rapid time constant of ~200 ms (ref. 15), we next tested the idea that HFS is associated with increases in extracellular adenosine. Using an amperometric biosensor, we found that adenosine abundance was increased as a function of both the frequency and the current amplitude of HFS (Fig. 1e). Furthermore, consistent with our ATP results, removal of extracellular Ca²⁺ significantly increased adenosine release (Fig. 1f). Slices exposed to the ecto-ATPase inhibitor ARL-67156 (6-*N,N*-diethyl-D-β,γ-dibromomethyleneATP; 50 μM) had reduced HFS-induced adenosine increase (Fig. 1g), suggesting that the adenosine originates primarily from the extracellular hydrolysis of ATP. The lack of complete inhibition suggests either inefficient blocking of extracellular ATP degradative enzymes or adenosine release by alternative pathways¹⁶.

To address whether adenosine contributes to the HFS-induced suppression of thalamic activity in the slice, thalamic neuron activity was recorded in current-clamp configuration during HFS delivery (125 Hz, 250 μA, 10 s, 32 °C) by a bipolar stimulating electrode located ~100 μm from the recorded neuron. Monosynaptic excitatory postsynaptic potentials (eEPSPs) were elicited by a separate stimulation electrode (Fig. 2a). HFS was associated with a significant reduction in the amplitude of eEPSPs that returned to prestimulation amplitude within ~5 s after cessation of HFS (Fig. 2a). The selective

¹Division of Glial Disease and Therapeutics, Department of Neurosurgery, University of Rochester, Rochester, New York 14642, USA. ²US National Institute of Diabetes and Digestive and Kidney Diseases, National Institutes of Health, Building 10, Room 4D51, Bethesda, Maryland 20892, USA. ³These authors contributed equally to this work. Correspondence should be addressed to L.B. (lane_bekar@urmc.rochester.edu) or M.N. (nedergaard@urmc.rochester.edu).

Received 23 April; accepted 29 November; published online 23 December 2007; doi:10.1038/nm1693

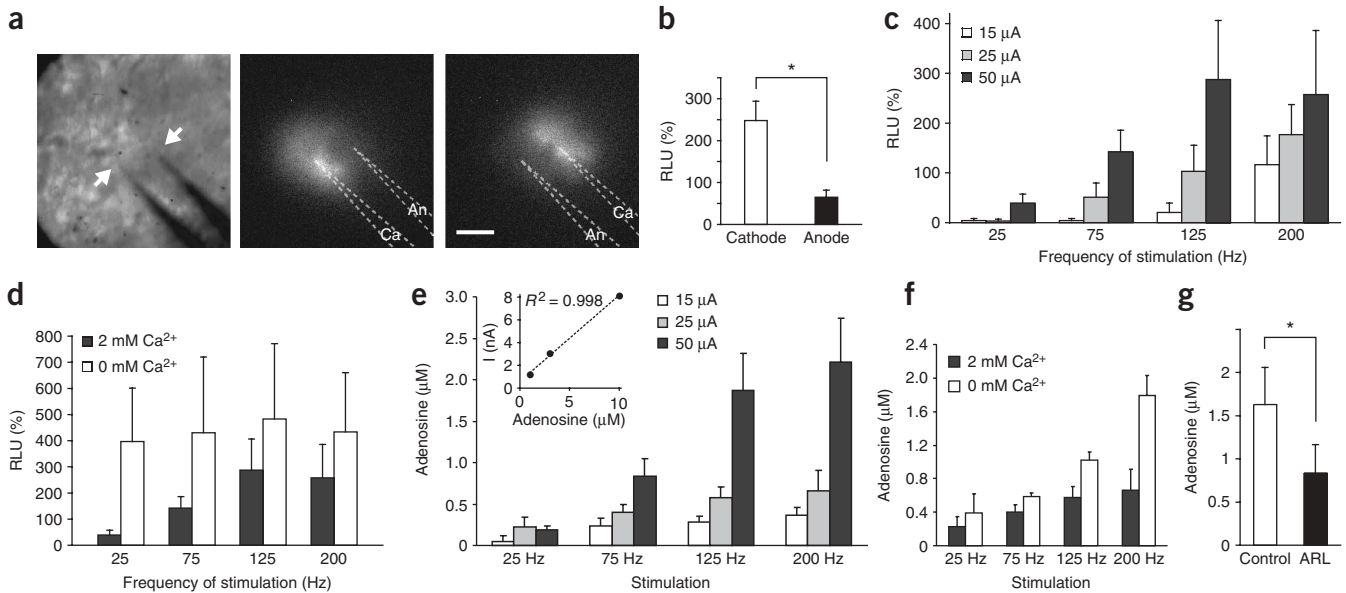


Figure 1 HFS triggers release of ATP and adenosine in thalamic slices. **(a)** Bioluminescence imaging of ATP release from thalamic slices. Bright-field image (left) of a bipolar electrode positioned to stimulate a thalamic slice. High-frequency stimulation (125 Hz, 50 μ A, 10 s) triggered ATP release from thalamic tissue in contact with the cathode (Ca; middle). ATP was released from the other pole of the electrode after the polarity of the electrode was changed (right). An, anode. Scale bar, 100 μ m. **(b)** Histogram comparing ATP release from the cathode versus the anode ($n = 7$, $*P = 0.002$, paired t -test). **(c)** ATP release as a function of amplitude and frequency of stimulation ($n = 4-6$, $P < 0.004$, two-way ANOVA). **(d)** Removal of extracellular Ca^{2+} increased ATP release at 50 μ A ($n = 3-6$, $P = 0.009$, two-way ANOVA). **(e)** Extracellular adenosine concentration increased as a function of amplitude and frequency of HFS (10 s) of thalamic slices ($n = 4$, $P < 0.001$, two-way ANOVA). Inset, example calibration for the adenosine sensor. The sensitivity limit was 0.1–1.0 μ M adenosine. **(f)** Removal of extracellular Ca^{2+} potentiated HFS-induced increases in extracellular adenosine ($n = 4$, $P < 0.001$, two-way ANOVA). **(g)** An ectonucleotidase inhibitor, ARL (50 μ M), reduced adenosine increases during HFS ($n = 6$, $P = 0.013$, paired t -test).

adenosine A1 receptor antagonist DPCPX potently attenuated the HFS-induced suppression of eEPSPs (Fig. 2a,b). This observation suggests that adenosine reversibly inhibits excitatory transmission in the thalamus during HFS.

As it has previously been shown that both axonal mechanisms and neurotransmitter depletion contribute to the antitremor effect of HFS (ref. 17), we also evaluated the contribution of A1 receptors to the depression of directly stimulated pathways. We evoked eEPSPs with the same stimulation electrode used for delivering HFS (Fig. 2c). Directly stimulated pathways showed a larger reduction in the amplitude of eEPSPs, and DPCPX attenuated this reduction after, but not during, HFS (Fig. 2c,d). Whereas eEPSPs recovered to prestimulation amplitudes in 26.75 ± 10.3 s in HFS-treated control slices, DPCPX (300 nM) antagonized the HFS-induced suppression of eEPSPs during the recovery phase, with eEPSPs recovering to prestimulation values in 12.4 ± 6.1 s. Thus, our observations suggest that adenosine A1 receptors augment synaptic mechanisms of depression in homosynaptic pathways and are responsible for the depression of heterosynaptic pathways. Of note, HFS was associated with a transient depolarization of the cell membrane (< 1 s) that resulted from synaptic release of glutamate, as administration of either the two glutamate receptor antagonists 2-amino-5-phosphonovaleric acid (APV) and 6-cyano-7-nitroquinoxaline-2,3-dione (CNQX), or the neurotoxin tetrodotoxin, effectively blocked HFS-induced depolarization (Supplementary Fig. 2 online).

To further analyze the role of adenosine in HFS, we studied the effect of perfusing thalamic slices with artificial cerebrospinal fluid (aCSF) containing 1–100 μ M adenosine. Adenosine suppressed the amplitude of eEPSPs by a maximum of 76.13% with a median

effective dose (ED_{50}) of 3.35 ± 0.75 μ M (Fig. 2e). The inhibitory effect of adenosine was mediated by A1 receptors because DPCPX (100 nM) reversibly attenuated the reduction (Fig. 2f). Additionally, 2-chloro-N6-cyclopentyladenosine (CCPA, 1.0 μ M), a selective adenosine A1 receptor agonist, mimicked the action of adenosine by potently depressing eEPSPs by $75.59 \pm 4.98\%$. Consistent with the direct amperometric measurements of adenosine (Fig. 1), the ecto-ATPase inhibitor ARL-67156 (50 μ M) attenuated HFS-induced depression of eEPSPs (ref. 18), suggesting that adenosine accumulation originated primarily from ATP hydrolysis (Fig. 2g). In contrast, the N-methyl-D-aspartic acid receptor antagonist APV (50 μ M) had no significant effect on eEPSP depression in response to HFS. Notably, HFS triggered a $101.75 \pm 13.13\%$ increase in eEPSPs in slices prepared from mice with deletion of adenosine A1 receptors¹⁹, whereas a reduction of eEPSPs of $32.91 \pm 7.43\%$ was evident in littermate controls ($A1ar^{+/+}$; Fig. 2g). Combined, the thalamic slice experiments provide direct evidence of roles for adenosine A1 receptors in depression of synaptic transmission during and after HFS, but they also confirm that axonal or synaptic mechanisms contribute to depression of directly stimulated pathways.

To address whether activation of adenosine receptors is an essential step in the depression of tremor in intact mice, we evaluated several mouse models of tremor, including treatment with tacrine, an anticholinesterase that produces parkinsonian side effects²⁰; lesioning of the nigrostriatal system by 6-hydroxydopamine (6-OHDA) injection into the medial forebrain bundle²¹; and treatment with the alkaloid harmaline to induce essential tremor^{22,23}. The model most amenable to pharmacological experimentation was the harmaline model, owing to its long-lasting tremor-producing effects (relative to those of

tacrine) and the lack of a need for surgical interventions that reduce the mouse yield (<10% of 6-OHDA-injected mice developed measurable tremor). Tremor activity was recorded either by electromyography (EMG) electrodes²⁴ or by placing the mouse on a load sensor²² and analyzing the power spectrum of the analog signal (Fig. 3a,b). Bilateral concentric bipolar stimulation electrodes were implanted in the thalamus, and the minimal efficient current amplitude of DBS was determined by methodically changing the stimulation parameters in harmaline-induced tremor (Fig. 3c). Tremor was suppressed immediately when therapeutic intensities of HFS were delivered, but it reappeared shortly (~ 5–10 s) after stimulation was discontinued. As DBS-mediated suppression shows rapid onset and recovery, we were able to evaluate it in the other two mouse models, which showed that HFS induces tremor suppression both transiently and with equal potency (Supplementary Fig. 3 online).

Before addressing adenosine's role in DBS-mediated tremor suppression, we first asked whether adenosine alone can dampen tremor

activity. We found that the blood-brain barrier-permeable adenosine A1 receptor antagonist DPCPX (4 mg/kg given intraperitoneally (i.p.)) significantly increased the power of the tremor induced by the alkaloid harmaline (Fig. 4a), indicating that endogenous adenosine is involved in dampening tremor activity. In addition, reverse microdialysis of adenosine or CCPA into the thalamus reduced tremor activity with a potency comparable to that of DBS (Fig. 4b). Unlike the effects of DBS, however, adenosine- and CCPA-mediated effects developed slowly over minutes, and tremor slowly reappeared upon discontinuation of microdialysis (Supplementary Fig. 4 online). Delivery of the γ -aminobutyric acid A (GABA_A) receptor agonist muscimol also reduced tremor activity, verifying the possible involvement of GABAergic mechanisms as previously suggested⁴ (Fig. 4b). Reverse microdialysis of the GABA_A receptor antagonist bicuculline resulted in hyperexcitability leading to generalized seizure activity (data not shown).

As endogenous adenosine and GABA mechanisms may actively suppress tremor, we addressed the hypothesis that additional adenosine

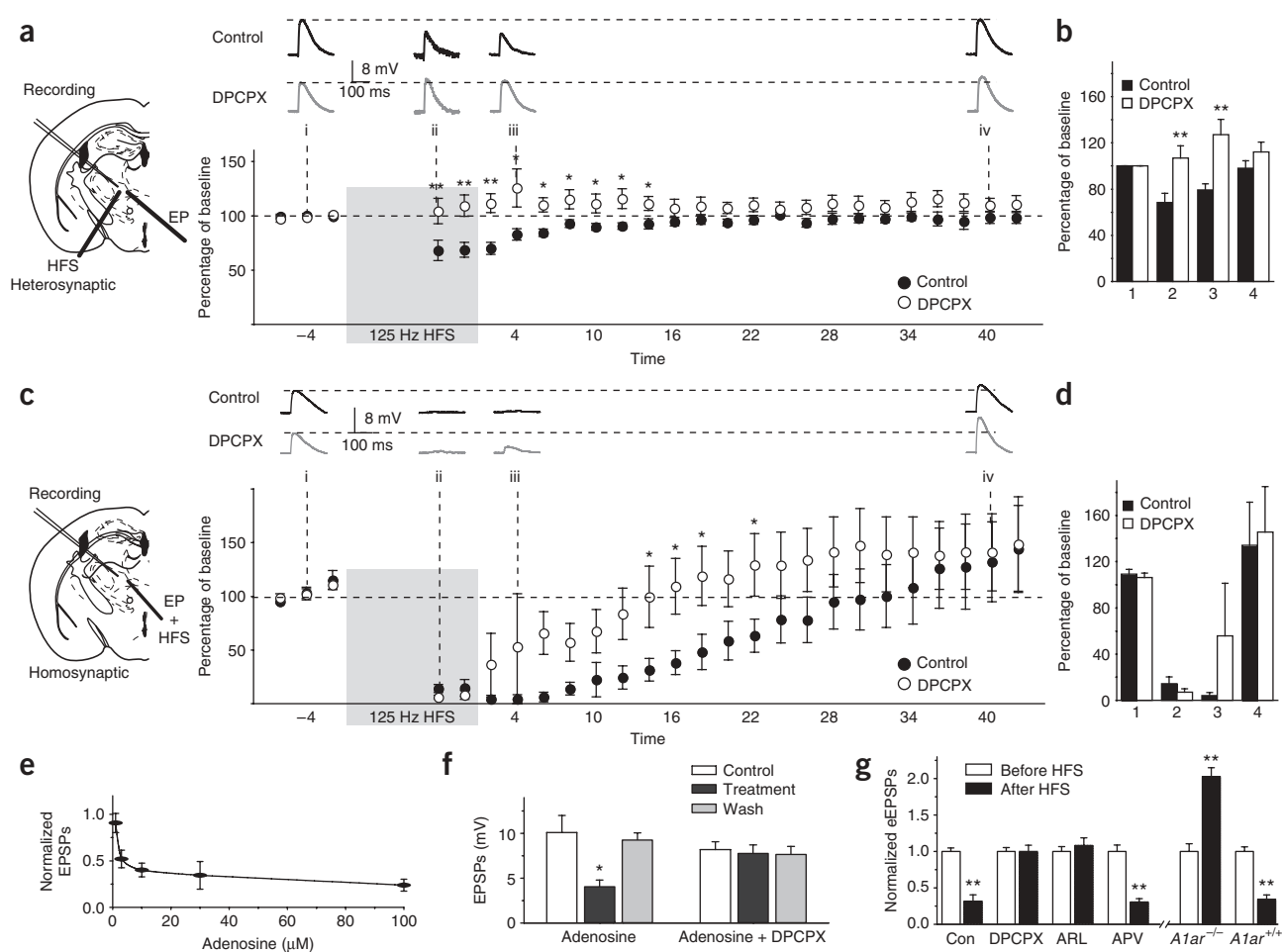


Figure 2 A1 receptor activation reduces excitatory transmission after HFS. (a) DPCPX attenuates HFS-induced depression of heterosynaptic pathways. Separate electrodes were used for delivery of HFS (125 Hz, 250 μ A, 100 μ s, 10 s, 32 $^{\circ}$ C) and evoked potentials (EP; 2.5 Hz; schematic). The amplitude of the evoked EPSPs (eEPSPs) was reduced during HFS, but DPCPX attenuated the depression of eEPSPs ($n = 5$, $*P < 0.05$, $**P < 0.001$; ANOVA with Holm-Sidak *post hoc* analysis). Examples of eEPSP profiles for each condition are illustrated above the graph. (b) Histogram comparing HFS induced depression of eEPSPs (average of 10 at 2.5 Hz) before (1), during (2), and at 4 s (3) and 40 s (4) after HFS of heterosynaptic pathways ($n = 5$, $**P < 0.001$, ANOVA with Holm-Sidak *post hoc* analysis compared to control). (c) DPCPX reduced depression of eEPSPs after, but not during, HFS of homosynaptic pathways ($n = 4$, $*P < 0.05$, ANOVA with Holm-Sidak *post hoc* analysis). (d) Histogram comparing HFS-induced depression of eEPSPs. (e) Adenosine depressed the amplitude of eEPSPs in a dose-dependent manner with an ED₅₀ of $3.35 \pm 0.75 \mu$ M. (f) Adenosine depression of eEPSPs is reversible ($n = 6$, $*P < 0.05$, paired *t*-test) and is blocked by DPCPX. (g) Pharmacology of HFS-mediated eEPSP reduction (250 μ A, 100 μ s, 5 s, 20 $^{\circ}$ C; $n = 9-12$, $**P < 0.001$, paired *t*-test).

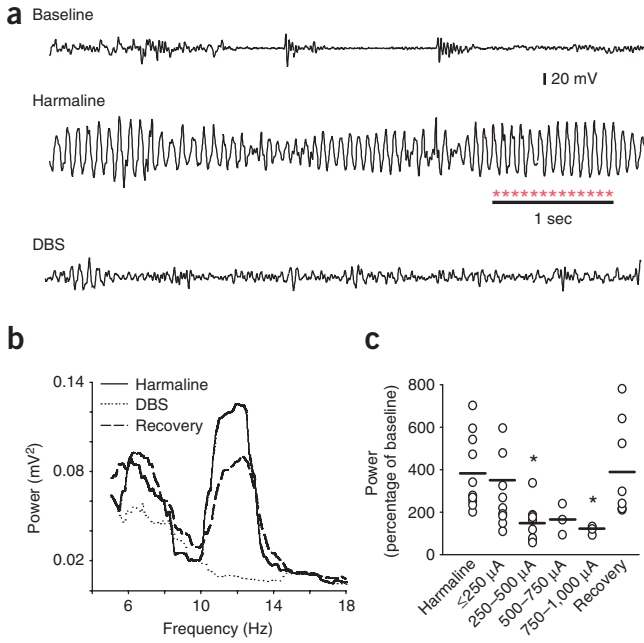


Figure 3 HFS reduces tremor power. **(a)** Representative recordings from a load sensor before (top) and after administration of harmaline (20 mg/kg; middle) and during HFS (200 μA , 125 Hz, 60 μs ; bottom). **(b)** Power spectrum analysis of traces from **a**. **(c)** Systematically increasing current intensity shows an amplitude-dependent suppression of tremor.

release in response to DBS aids in the DBS-mediated tremor suppression. Thus, we measured the range of stimulation intensity values corresponding to the therapeutic window of mice exposed to harmaline (Fig. 4c). The window was defined as the minimum stimulation amplitude that reduced tremor (>50% reduction in power spectrum) at the lower range and the lowest current amplitude that triggered involuntary movements at the higher range. Typically, DBS reduced tremor with a threshold current of ~400 μA , and involuntary

movements were triggered when the current was increased by an additional 200–300 μA (Fig. 4c). Systemic administration of APV and CNQX (10 mg/kg each i.p.) reduced overall locomotion but had no effect on the ability of DBS to reduce harmaline-induced tremor activity (Fig. 4c). However, the threshold for inducing involuntary movements was increased with APV and CNQX treatment, supporting the notion that glutamate release is responsible for involuntary movements²⁵. APV plus CNQX significantly expanded the range of the therapeutic window, from $280 \pm 80\ \mu A$ to $710 \pm 210\ \mu A$ ($P = 0.027$, unpaired t -test). In contrast, mice treated with the adenosine A1 receptor antagonist DPCPX (4 mg/kg i.p.), or mutant mice lacking the A1 receptor, developed involuntary movements at stimulation intensities below the therapeutic range (Fig. 4c). Thus, side effects expressed as involuntary movements prevented the use of DBS in mice lacking functional A1 receptors. Notably, all A1 receptor-null mice exposed to DBS showed generalized seizures at stimulation intensities higher than 500 μA . These mice were killed for histological verification of electrode positioning after having experienced 30 min of status epilepticus. In contrast, seizure was never induced at considerably higher stimulation intensities (>700 μA) in either of the other groups.

As mentioned, if the intensity of stimulation is increased beyond the therapeutic range, mice show repetitive, involuntary movements of the upper limbs and jaw. Such involuntary movements are comparable to those of patients typically experiencing unpleasant parasthesia when the intensity of DBS exceeds the therapeutic level. In mice, it is not possible to determine whether involuntary movements are aversive reactions to painful parasthesia or, alternatively, a result of current spread triggering tetanic motor unit discharge²⁵. Nevertheless, the involuntary movements were clearly side effects caused by supra-threshold stimulation. As such, the threshold for involuntary movements can be used to evaluate the role of adenosine in limiting side effects evoked by DBS in the presence and absence of tremor. We found that DPCPX reduced the threshold for DBS-induced involuntary movements in the absence of tremor (Fig. 4d), suggesting that release of endogenous adenosine reduces the spread of excitation produced by DBS. Of note, when stimulation was repeated in the same

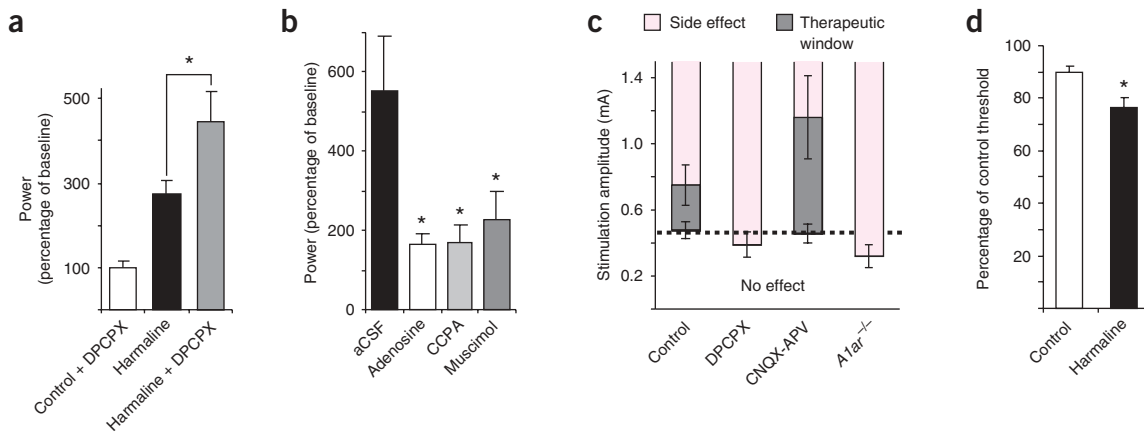


Figure 4 Antitremor effect of HFS is mediated by A1 receptor activation. **(a)** DPCPX had no effect in a nontremoring mouse, but significantly increased the harmaline-induced tremor ($n = 3$ –13, $*P < 0.05$, unpaired t -test). **(b)** Effect of adenosine, the adenosine A1 agonist CCPA and the GABA_A agonist muscimol on harmaline-induced tremor. The peak reduction of tremor, which typically occurred after several minutes of agonist perfusion, was compared to baseline tremor in the same mouse ($n = 3$ –5, $*P < 0.05$, unpaired t -test). **(c)** The therapeutic window of DBS on harmaline-induced tremor in control ($n = 10$), APV-CNQX ($n = 5$), DPCPX ($n = 5$) and A1 receptor-null mice ($n = 3$) were compared. ‘No effect’ represents stimulation intensities below threshold for suppressing tremor activity. **(d)** DPCPX effects on the threshold for dyskinetic movements in mice under control conditions and with harmaline-induced tremor.

mice after administration of harmaline, DPCPX reduced the threshold for side effect induction significantly more than it did in the absence of tremor (Fig. 4d). These observations suggest the possibility that endogenous background adenosine levels are higher in mice with tremor compared to control mice.

Combined, the *in vivo* experiments show that nonsynaptic release of ATP and the subsequent activation of adenosine A1 receptors are crucial in DBS-induced reduction of tremor by limiting excitatory side effects (involuntary movements). Pharmacological or genetic inactivation of adenosine A1 receptors prevented the therapeutic effect of DBS owing to a substantial lowering of the threshold for excitatory side effects. Conversely, intrathalamic infusion of adenosine and A1 receptor agonists mimicked the beneficial effects of DBS. To our knowledge, this is the first evidence that DBS is associated with the release of ATP and adenosine and that A1 receptors have a central role in reducing DBS-evoked side effects, thereby permitting the delivery of HFS without inducing seizure. Although previous studies have focused on neuronal or synaptic alterations associated with DBS, (reviewed in ref. 26), this study suggests that nonsynaptic mechanisms involving the activation of A1 receptors work in concert with transmitter depletion to suppress tremor activity. Recent work indicates that astrocytes are important in regulating the extracellular concentration of adenosine, underlining the need for additional studies defining the involvement of astrocytes in DBS (refs. 27,28).

We conclude that the activation of thalamic adenosine A1 receptors is key in the prevention of DBS-mediated excitatory side effects and acts in conjunction with GABA and direct axonal mechanisms in DBS-induced reduction of tremor.

METHODS

Slice preparation and electrophysiology. We cut thalamic slices (300 μm) from 14–21-day-old FVB/NJ or adenosine A1 receptor–mutant mouse¹⁹ pups on a Vibratome (TPI) in an ice-cold cutting solution containing 2.5 mM KCl, 1.25 mM NaH_2PO_4 , 10 mM MgSO_4 , 5 mM CaCl_2 , 10 mM glucose, 26 mM NaHCO_3 and 230 mM sucrose, and the solution was gassed with 5% CO_2 and 95% O_2 . We incubated the slices for a minimum of 1 h in aCSF at room temperature and transferred them to a recording chamber perfused with aCSF at a temperature of 22 °C or 32 °C. The aCSF contained 126 mM NaCl, 2.5 mM KCl, 1.25 mM NaH_2PO_4 , 2 mM MgCl_2 , 2 mM CaCl_2 , 10 mM glucose and 26 mM NaHCO_3 at pH 7.4 and was gassed with 5% CO_2 and 95% O_2 . We obtained whole-cell current clamp recordings with a 700B MultiClamp amplifier (Axon Instruments) from the ventrolateral thalamus²⁹. We placed concentric bipolar stimulating electrodes (FHC) \sim 100–400 μm ventromedial to the patched neuron. We delivered HFS (60 μs ; 15, 25 or 50 μA ; 25, 75, 125 or 200 Hz) through a constant isolated current source (an ISO-Flex isolator with a Master-8-vp stimulator; AMPI). For measurement of eEPSPs, we blanked the artifacts (and staggered them for heterosynaptic effects) to allow continuous observation of the 2.5-Hz signal. We detected adenosine by amperometric measurements with needle-shaped biosensors held at 500 mV (Sarissa Biomedical). We carried out calibration at the beginning and end of each experiment in the bath above the slice preparation. We obtained measurements \sim 100 μm from the stimulation electrode in the thalamic slice. We performed separate experiments with an inosine biosensor to verify that inosine constituted less than 10% of the observed adenosine responses (data not shown).

Mouse preparation. Male FVB/NJ or A1 receptor–mutant mice¹⁹ (8–10 weeks old) were anesthetized with ketamine and xylazine (60 mg/kg and 10 mg/kg, respectively, i.p.). Knockout mice were the offspring of heterozygous (*A1ar*^{+/-}) mice on a 129/SVJ/C57BL/6 background. We used littermate wild-type mice (*A1ar*^{+/+}) as controls in all experiments. For imaging experiments, we intubated and artificially ventilated the mice with a small-animal ventilator (SAR-830, CWE; 100 breaths/min and 0.3–0.4 ml/breath). We cannulated a femoral artery for monitoring of blood pressure and blood gas pressure (pCO₂, pO₂ and pH) with a blood gas analyzer (Rapiddlab 248, Bayer, samples 40 μl), and we

maintained body temperature at 37 °C with a heating blanket (T/PUMP, Gaymer). We glued a custom-made metal plate to the skull with dental cement and did a craniotomy (3 mm in diameter) over the left hemisphere of the brain. For tremor experiments, we exposed the skull and implanted concentric bipolar microelectrodes (SNE-100, KOPF) or microdialysis probes (Bioanalytical Systems) into the ventrolateral thalamic nucleus at the following coordinates from bema—anterior-posterior, -1.4 mm; lateral, \pm 0.9 mm; ventral, -3.7 mm—and attached them to the skull with dental cement. In a subset of these mice, EMG electrodes were placed in the occipital muscles for measurement of tremor activity. All experiments were approved by the Institutional Animal Care and Use Committee of the University of Rochester.

Imaging. We performed two-photon imaging of calcium waves as previously described¹⁴. For ATP measurements, we included luciferase (0.132 mg/ml) and luciferin (0.332 mg/ml) in an aCSF solution delivered at a rate of \sim 2–3 ml/min to the thalamic slice (Minipump RT-202, VWR)⁸. We imaged photon production from the exposed cortex in response to stimulation with a liquid nitrogen-cooled charge-coupled device camera⁸.

Tremor models. We administered harmaline i.p. 20 min before DBS (20–30 mg/kg)^{22,23}. We injected 6-OHDA (3 $\mu\text{g}/\mu\text{l}$ in saline containing 0.1% ascorbic acid) into the right median forebrain bundle (anterior-posterior, -1.2 mm; lateral, \pm 1.1 mm; ventral, -5.0 mm in a volume of 2 μl)²¹ in mice anesthetized with urethane (1.6 g/kg). We included only mice that developed body tremor in the study. We administered tacrine in a dose of 2.5 mg/kg i.p. and induced a robust jaw response with the peak frequency within the 3–5 Hz range²⁰. After allowing 24 h of recovery from electrode or microdialysis probe implantation, we delivered stimulation through a constant isolated current source. Twenty-four hours after implantation, we perfused microdialysis probes with the perfusion buffer at a rate of 2 $\mu\text{l}/\text{min}$ with a microinjection pump (Harvard Apparatus). We added adenosine (1–10 mM) or CCPA (10–500 μM) to the perfusion buffer. We recorded tremor in awake, freely moving mice either with EMG electrodes or with the Convuls-1 pressure transducer (Columbus Instruments). We used power spectrum analysis to compare tremor activity in awake, freely moving mice before, during and after DBS or delivery of adenosine agonists by the microdialysis probes²⁴. After experimentation, we perfusion-fixed and sectioned the mice on a vibratome for confirmation of electrode or microdialysis probe placement (Supplementary Fig. 5 online).

Tremor electrode properties. The electrodes implanted in tremor-affected individuals have four contacts with a total surface area of 0.24 cm², an impedance of \sim 500 Ohm and an upper limit of 30 $\mu\text{C}/\text{cm}^2$ in charge density³⁰. In mice, we used electrodes with a smaller tip (diameter 0.0055–0.250 mm, surface area 0.001–0.05 mm²) and adjusted the current amplitude to obtain a charge density within the range of \sim 1–10 $\mu\text{C}/\text{cm}^2$.

Statistical analyses. Data are presented as means \pm s.e.m. We performed single comparisons with paired and unpaired *t*-tests. We compared multiple groups using two-way analysis of variance (ANOVA) with the Holm-Sidak method for analysis of significance between groups. A *P* value of less than 0.05 was considered significant.

Note: Supplementary information is available on the Nature Medicine website.

ACKNOWLEDGMENTS

We thank S. Goldman and E. Vates for comments on the manuscript. This work was supported by the Mathers Charitable Foundation; National Institutes of Health grants NS30007, NS39559 and NS050315; the Adelson Program in Neural Repair and Regeneration; The Philip-Morris Organization; the New York State Spinal Cord Injury Research Board and the Canadian Institutes of Health Research.

Published online at <http://www.nature.com/naturemedicine>
Reprints and permissions information is available online at <http://npg.nature.com/reprintsandpermissions>

- Lozano, A.M. & Eltahawy, H. How does DBS work? *Suppl. Clin. Neurophysiol.* **57**, 733–736 (2004).
- Marks, W.J. Deep brain stimulation for dystonia. *Curr. Treat. Options Neurol.* **7**, 237–243 (2005).

3. Hamani, C. *et al.* Deep brain stimulation for chronic neuropathic pain: long-term outcome and the incidence of insertional effect. *Pain* **125**, 188–196 (2006).
4. McIntyre, C.C., Savasta, M., Walter, B.L. & Vitek, J.L. How does deep brain stimulation work? Present understanding and future questions. *J. Clin. Neurophysiol.* **21**, 40–50 (2004).
5. Mayberg, H.S. *et al.* Deep brain stimulation for treatment-resistant depression. *Neuron* **45**, 651–660 (2005).
6. Wichmann, T. & DeLong, M.R. Deep brain stimulation for neurologic and neuropsychiatric disorders. *Neuron* **52**, 197–204 (2006).
7. Louis, E.D. *et al.* Semiquantitative study of current coffee, caffeine and ethanol intake in essential tremor cases and controls. *Mov. Disord.* **19**, 499–504 (2004).
8. Wang, X. *et al.* P2X7 receptor inhibition improves recovery after spinal cord injury. *Nat. Med.* **10**, 821–827 (2004).
9. Arcuino, G. *et al.* Intercellular calcium signaling mediated by point-source burst release of ATP. *Proc. Natl. Acad. Sci. USA* **99**, 9840–9845 (2002).
10. Benabid, A.L. *et al.* Chronic electrical stimulation of the ventralis intermedialis nucleus of the thalamus as a treatment of movement disorders. *J. Neurosurg.* **84**, 203–214 (1996).
11. McIntyre, C.C. & Grill, W.M. Extracellular stimulation of central neurons: influence of stimulus waveform and frequency on neuronal output. *J. Neurophysiol.* **88**, 1592–1604 (2002).
12. Cotrina, M.L. *et al.* Connexins regulate calcium signaling by controlling ATP release. *Proc. Natl. Acad. Sci. USA* **95**, 15735–15740 (1998).
13. Burnstock, G. Physiology and pathophysiology of purinergic neurotransmission. *Physiol. Rev.* **87**, 659–797 (2007).
14. Wang, X. *et al.* Astrocytic Ca²⁺ signaling evoked by sensory stimulation *in vivo*. *Nat. Neurosci.* **9**, 816–823 (2006).
15. Dunwiddie, T.V., Diao, L. & Proctor, W.R. Adenine nucleotides undergo rapid, quantitative conversion to adenosine in the extracellular space in rat hippocampus. *J. Neurosci.* **17**, 7673–7682 (1997).
16. Wall, M.J. & Dale, N. Auto-inhibition of parallel fibre–Purkinje cell synapses by activity dependent adenosine release. *J. Physiol. (Lond.)* **581**, 553–565 (2007).
17. Anderson, T.R., Hu, B., Iremonger, K. & Kiss, Z.H. Selective attenuation of afferent synaptic transmission as a mechanism of thalamic deep brain stimulation–induced tremor arrest. *J. Neurosci.* **26**, 841–850 (2006).
18. Gomes, P., Srinivas, S.P., Van Driessche, W., Vereecke, J. & Himpens, B. ATP release through connexin hemichannels in corneal endothelial cells. *Invest. Ophthalmol. Vis. Sci.* **46**, 1208–1218 (2005).
19. Sun, D. *et al.* Mediation of tubuloglomerular feedback by adenosine: evidence from mice lacking adenosine 1 receptors. *Proc. Natl. Acad. Sci. USA* **98**, 9983–9988 (2001).
20. Cousins, M.S., Carriero, D.L. & Salamone, J.D. Tremulous jaw movements induced by the acetylcholinesterase inhibitor tacrine: effects of antiparkinsonian drugs. *Eur. J. Pharmacol.* **322**, 137–145 (1997).
21. Jolicœur, F.B., Rivest, R. & Drumheller, A. Hypokinesia, rigidity, and tremor induced by hypothalamic 6-OHDA lesions in the rat. *Brain Res. Bull.* **26**, 317–320 (1991).
22. Martin, F.C., Thu Le, A. & Handforth, A. Harmaline-induced tremor as a potential preclinical screening method for essential tremor medications. *Mov. Disord.* **20**, 298–305 (2005).
23. Wilms, H., Sievers, J. & Deuschl, G. Animal models of tremor. *Mov. Disord.* **14**, 557–571 (1999).
24. Milner, T.E., Cadoret, G., Lessard, L. & Smith, A.M. EMG analysis of harmaline-induced tremor in normal and three strains of mutant mice with Purkinje cell degeneration and the role of the inferior olive. *J. Neurophysiol.* **73**, 2568–2577 (1995).
25. Boulet, S. *et al.* Subthalamic stimulation–induced forelimb dyskinesias are linked to an increase in glutamate levels in the substantia nigra pars reticulata. *J. Neurosci.* **26**, 10768–10776 (2006).
26. Perlmutter, J.S. & Mink, J.W. Deep brain stimulation. *Annu. Rev. Neurosci.* **29**, 229–257 (2006).
27. Zhang, J.M. *et al.* ATP released by astrocytes mediates glutamatergic activity–dependent heterosynaptic suppression. *Neuron* **40**, 971–982 (2003).
28. Pascual, O. *et al.* Astrocytic purinergic signaling coordinates synaptic networks. *Science* **310**, 113–116 (2005).
29. Jiang, L., Xu, J., Nedergaard, M. & Kang, J. A kainate receptor increases the efficacy of GABAergic synapses. *Neuron* **30**, 503–513 (2001).
30. Kuncel, A.M. & Grill, W.M. Selection of stimulus parameters for deep brain stimulation. *Clin. Neurophysiol.* **115**, 2431–2441 (2004).